Proceedings of the 11th ICPMG 2026
11th International Conference on Physical Modelling in Geotechnics
8-12 June 2026, Zurich, Switzerland

Acoustic Emission as an indicator of sand deformation in drained triaxial tests

S.A. Solh, S. Abdelaziz
Virginia Tech, Blacksburg, VA, USA, saadallahsolh@vt.edu, saziz@vt.edu

ABSTRACT: AE is a non-destructive method that captures high-frequency waves from micromechanical events in soils, offering insight into deformation onset and proximity to failure. This study evaluates AE as an early-warning indicator using drained triaxial tests on Ottawa sand at two relative densities, 40% and 85%. A conventional triaxial apparatus instrumented with resonant sensors embedded in the end caps recorded acoustic activity during creep and shear. AE intensity was quantified by signal strength (SS) and compared with deviatoric stress, axial strain, and volumetric strain. During creep, the SS rate was near zero, then increased immediately at the onset of shearing, demonstrating sensitivity to the start of deformation. Up to peak strength, both densities exhibited similar SS rates despite different stress levels, indicating AE activity is more closely tied to strain state than to absolute stress. Beyond peak, deviatoric stress softened while the SS rate remained elevated and increasingly intermittent, consistent with persistent localized shearing; the denser specimen showed a larger post-peak rise, aligning with stronger dilation and contact interlocking/breakage. Overall, the results indicate that AE can both detect the initiation of deformation and qualitatively gauge proximity to peak and subsequent transition toward residual strength, supporting its use for early-warning applications in granular soils.

1 INTRODUCTION

Granular soils govern the performance and safety of many geotechnical systems, yet their macroscopic response emerges from discrete, nonlinear interactions at grain contacts such as rearrangement, sliding/rolling friction, force-chain formation and collapse, and occasional crushing (Been & Jefferies, 1985; Li et al., 2009; Wan & Nicot, 2010). Acoustic emission (AE) monitoring offers a direct window into these micromechanical processes by capturing transient high-frequency waves generated as strain energy is released at contacts (Koerner & Lord, 1974; Pollock, 1968). In sands, AE sources have been linked to contact slip and rolling (Koerner et al., 1976; Liu et al., 2022; Smith & Dixon, 2019b; Solh & Abdelaziz, 2024), fabric reorganization within the force network (Michlmayr et al., 2012), and particle damage (Mao & Towhata, 2015); fluid effects (e.g., seepage or undrained pore-pressure transients) can further modulate the signal (Hung et al., 2009; Solh et al., 2025).

AE is well established in other disciplines, such as bridges (Behnia et al., 2014), aircraft (Grigg et al., 2021), and pipeline systems (Lu & Wilson, 2012), with multiple standards, but its use in geotechnical engineering remains less mature. Early field applications by Koerner et al. (1981) monitored dams, embankments, and foundations, showing AE activity increasing as failure approached, albeit with primarily qualitative interpretation. More recently, Smith et al. (2018) Slope ALARMS demonstrated AE's capability for slope monitoring, including relationships between AE rate and deformation rate. Nevertheless, two practical questions remain central to early-warning in soils: (i) how reliably AE indicates the onset of deformation, and (ii) how AE evolves as the material approaches and passes peak strength toward residual.

This paper evaluates these questions using drained triaxial tests on Ottawa sand. We assess the feasibility of AE for detecting the onset of movement, operationally, the start of the shear phase following creep, and for gauging deformation progression by comparing AEs against conventional mechanical measurements. We further examine how relative density influences AE response. The findings are intended to inform analysis choices and support the eventual translation of AE methods from controlled laboratory settings to field applications.

2 METHODOLOGY

2.1 Material and Testing Procedure

Ottawa sand (20/30 mesh) was used in this study. It is classified as a poorly graded sand (SP) per the Unified Soil Classification System (USCS), with its grain-size distribution shown in Figure 1. The sand has a specific gravity of 2.65 and minimum and maximum void ratios of 0.49 and 0.73, respectively. A summary of the physical properties of the sand is provided in Table 1.

Table 1: Physical properties of Ottawa sand (20/30 Mesh)

Property	Value
Specific gravity, Gs	2.65
Mean particle diameter, D_{50} (mm)	0.60
Coefficient of uniformity, C_u	1.36
Coefficient of curvature, C_c	0.90
Maximum void ratio, e_{max}	0.73
Minimum void ratio, e_{min}	0.49

Two cylindrical specimens (100.6 mm diameter, 215.3 mm height) were prepared to target relative densities of 40% and 85% using the Undercompaction method (Ladd, 1978). Specimens were flushed with CO_2 to accelerate saturation (Chaney et al., 1979), followed by back-pressure saturation to 550 kPa while maintaining a constant effective confining stress of 35 kPa, achieving B > 0.95. Each specimen was then isotropically consolidated to a confining pressure of 300 kPa and subsequently sheared under drained conditions at a strain rate of 1%/h. AE signals were recorded continuously during the consolidation and shear phases.

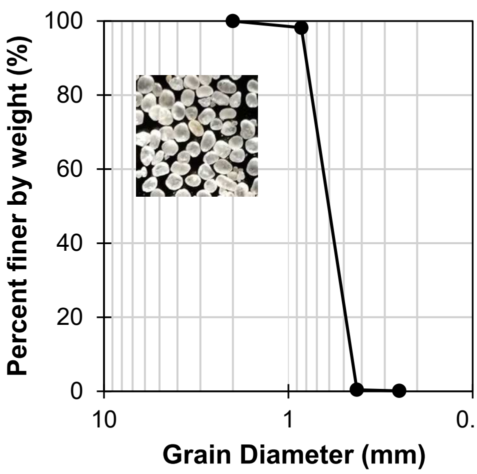

Figure 1. Grain-size distribution of Ottawa sand (20/30 mesh).

2.2 Acoustic-Enabled Triaxial System

A conventional triaxial apparatus was modified by embedding two AE sensors in the top and bottom end caps (Figure 2). The sensors (ISPK6IUC, Mistras Group) are resonant-type, sensitive over 10–100 kHz with a nominal resonance at 60 kHz and include integrated 26 dB preamplifiers to improve signal-to-noise ratio. Data were sampled at 1 MHz to prevent aliasing (Smith, 1997), and a 10–100 kHz digital band-pass filter was applied to suppress low-frequency background noise and out-of-band high-frequency content.

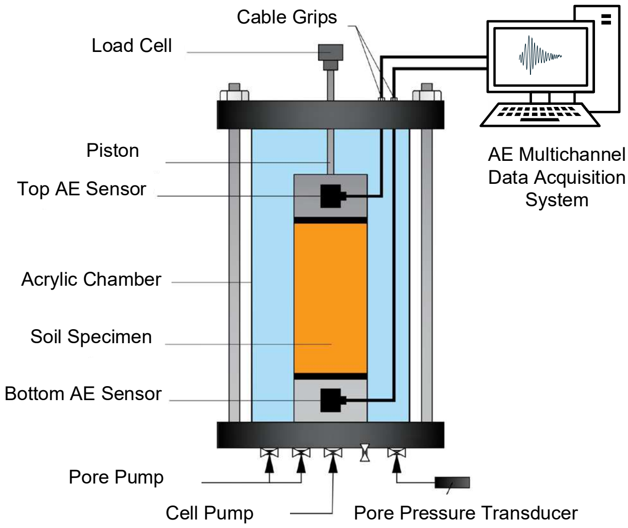

Figure 2. Schematic of the AE-enabled triaxial test setup with sensors embedded in the top and bottom end caps.

2.3 AE Acquisition Method and Parameter

The hit-based method was used to analyze the recorded AE waveforms. A fixed threshold of 45 dB (re 1 µV at the sensor input) was set; when the rectified signal first exceeds this threshold, a new hit is initiated. A hit terminates once the signal remains below the threshold for the Hit Definition Time (HDT), and a subsequent Hit Lockout Time (HLT) prevents immediate re-triggering. Based on prior system calibration, HDT = HLT = 600 µs.

The intensity of each hit was quantified by the signal strength (SS), computed using Eq.1 and is expressed in µV.s.

$$SS = \sum_{FTC}^{LTC} |V_i| . \Delta t \qquad (1)$$

where, V_i is the value of the digitized voltage at sample i, Δt is the sampling interval (1µs for 1MHz sampling rate), and FTC/LTC denote the first/last threshold crossings of the hit.

3 RESULTS AND DISCUSSION

Figure 3 illustrates the evolution of deviatoric stress (σ_d), volumetric strain (ε_v), and signal strength (SS) rate (computed in 60-s windows from the bottom-cap sensor) with respect to time and axial strain (ε_a) during the creep and shear phases. After isotropic consolidation and dissipation of excess pore pressure, the creep phase began with negligible volumetric change and zero deviatoric stress (Figure 3b). During drained shear, the denser specimen (Dr = 85%) reached a higher peak strength than the looser specimen (Dr = 40%), followed by softening toward a similar residual strength at large strain (Figure 3a). Both specimens exhibited slight initial contraction followed by dilation, with greater dilation at higher relative density (Figure 3b).

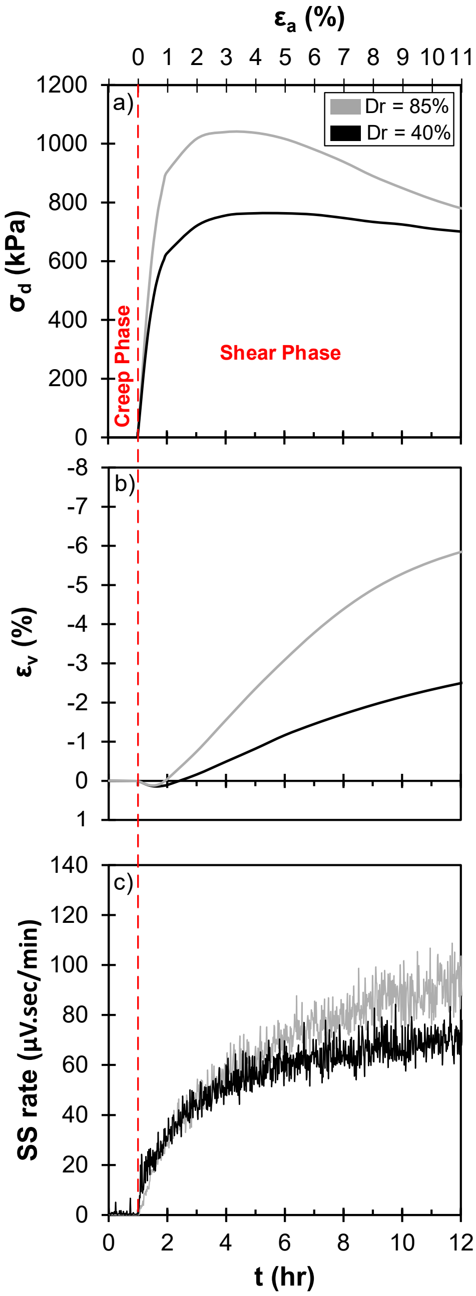

Figure 3. Evolution of (a) deviatoric stress, (b) volumetric strain, and (c) signal-strength (SS) rate for Ottawa sand at relative densities of 40% and 85% during the creep and shear phases.

In terms of AE response, the SS rate was very low during creep, then increased markedly once shearing commenced, indicating sensitivity to the onset of deformation (Figure 3c). The SS rate showed no clear inflection at the contractive–dilative transition. Beyond peak strength, deviatoric strerss softens while the SS rate remains elevated and increasingly intermittent, consistent with persistent localized shearing and continued contact rearrangement. The absence of a pronounced peak in SS rate aligns with the "Type 2" behavior described by Smith and Dixon (2019a), in which no clear peak accompanies the transition from contractive to dilative response.

Up to peak stress, both specimens produced comparable emission rates despite the higher stresses in the dense specimen, implying that the SS rate is more strain- than stress-controlled; after peak, the dense specimen shows a greater increase in SS rate, consistent with stronger dilation and contact interlocking/breakage. Overall, the results suggest that AE reflects the evolving strain level, with increased emissions as the soil approaches its ultimate capacity , consistent with observations in concrete, steel, and rock materials (Wang et al., 2023; Zhang et al., 2025).

4 CONCLUSIONS

This paper demonstrates that AE technique is a practical indicator of both deformation onset and proximity to failure in granular material. During creep, the SS rate remains near zero, but it increases immediately with the start of shearing showing that AE captures the initiation of micro-slip and fabric rearrangement.

Up to peak strength, specimens at Dr = 40% and 85% produce comparable SS rates despite different stress levels, implying that AE activity is more closely tied to the strain state than to absolute stress. Beyond peak strength, deviatoric stress softens while the SS rate remains elevated and increasingly intermittent, consistent with persistent localized shearing and continued contact rearrangement; the denser specimen shows a larger post-peak rise. Taken together, these trends indicate that AE can 1) flag the early start of deformation and 2) provide a qualitative gauge of closeness to peak and transition toward residual strength, supporting its use for early-warning applications in granular soils.

Future research should examine the influence of soil type and deformation rate on AE response, extend the application of the technique to cohesive soils, and validate AE-based indicators in largerscale physical models to bridge laboratory observations with field-scale geotechnical systems.

ACKNOWLEDGEMENTS

This material is based upon work supported by the Broad Agency Announcement Program and the Cold Regions Research and Engineering Laboratory (ERDC-CRREL) under Contract No. W913E522C0001. Any opinions, findings, and conclusions, or recommendations expressed in this material are those of the author(s) and do not necessarily reflect the views of the Broad Agency Announcement Program and ERDC-CRREL.

REFERENCES

Been, K., & Jefferies, M. G. (1985). A state parameter for sands. *Géotechnique*, *35*(2), 99-112. https://doi.org/10.1680/geot.1985.35.2.99

Behnia, A., Chai, H. K., & Shiotani, T. (2014). Advanced structural health monitoring of concrete structures with the aid of acoustic emission. *Construction and Building Materials*, *65*, 282-302. https://doi.org/https://doi.org/10.1016/j.conbuildmat.2014.04.103

Chaney, R., Stevens, E., & Sheth, N. (1979). Suggested Test Method for Determination of Degree of Saturation of Soil Samples by B Value Measurement. *Geotechnical Testing Journal*, *2*(3), 158-162. https://doi.org/10.1520/gtj10448j

Grigg, S., Pullin, R., Pearson, M., Jenman, D., Cooper, R., Parkins, A., & Featherston, C. A. (2021). Development of a low-power wireless acoustic emission sensor node for aerospace applications. *Structural control and health monitoring*, *28*(4). https://doi.org/10.1002/stc.2701

Hung, M.-H., Lauchle, G. C., & Wang, M. C. (2009). Seepage-Induced Acoustic Emission in Granular Soils. *Journal of Geotechnical and Geoenvironmental Engineering*, *135*(4), 566-572. https://doi.org/doi:10.1061/(ASCE)1090-0241(2009)135:4(566)

Koerner, R. M., Curran, J. W., McCabe, W. M., & Lord, A. E. (1976). Acoustic Emission Behavior of Granular Soils. *Journal of the Geotechnical Engineering Division*, *102*(7), 761-773. https://doi.org/doi:10.1061/AJGEB6.0000297

Koerner, R. M., & Lord, A. E. (1974). Acoustic emissions in stressed soil samples. *The Journal of the Acoustical Society of America*, *56*(6), 1924-1927. https://doi.org/10.1121/1.1903538

Koerner, R. M., McCabe, W. M., & Lord, A. E. (1981). Acoustic Emission Behavior and Monitoring of Soils. In (pp. 93-141). ASTM International. https://doi.org/10.1520/STP28343S

Ladd, R. S. (1978). Preparing Test Specimens Using Undercompaction. *Geotechnical Testing Journal*, *1*(1), 16-23. https://doi.org/10.1520/GTJ10364J

Li, X., Yu, H. S., & Li, X. S. (2009). Macro–micro relations in granular mechanics. *International Journal of Solids and Structures*, *46*(25-26), 4331-4341. https://doi.org/https://doi.org/10.1016/j.ijsolstr.2009.08.018

Liu, Z.-m., Jiang, Y., Wang, D.-j., & Fu, Y.-j. (2022). Four types of acoustic emission characteristics during granular stick-slip evolution. *Journal of Mountain Science*, *19*(1), 276-288. https://doi.org/10.1007/s11629-021-7012-z

Lu, Z., & Wilson, G. V. (2012). Acoustic Measurements of Soil Pipeflow and Internal Erosion. *Soil Science Society of America Journal*, *76*(3), 853-866. https://doi.org/10.2136/sssaj2011.0308

Mao, W., & Towhata, I. (2015). Monitoring of single-particle fragmentation process under static loading using acoustic emission. *Applied Acoustics*, *94*, 39-45. https://doi.org/https://doi.org/10.1016/j.apacoust.2015.02.007

Michlmayr, G., Cohen, D., & Or, D. (2012). Sources and characteristics of acoustic emissions from mechanically stressed geologic granular media — A review. *Earth-Science Reviews*, *112*(3), 97-114. https://doi.org/https://doi.org/10.1016/j.earscirev.2012.02.009

Pollock, A. A. (1968). Stress-wave emission — a new tool for industry. *Ultrasonics*, *6*(2), 88-92. https://doi.org/10.1016/0041-624X(68)90199-6

Smith, A., & Dixon, N. (2019a). Acoustic emission behaviour of dense sands. *Géotechnique*, *69*(12), 1107-1122. https://doi.org/10.1680/jgeot.18.P.209

Smith, A., & Dixon, N. (2019b). Acoustic emission generated by glass beads in compression and shearing. *Granular Matter*, *21*(4), 92. https://doi.org/10.1007/s10035-019-0944-0

Smith, A., Dixon, N., Flint, J. A., Khanna, R., Clark, B., & Andjelkovic, M. (2018). An acoustic emission landslide early warning system for communities in low-income and middle-income countries. *Landslides*, *15*(8), 1631-1644. https://doi.org/10.1007/s10346-018-0977-1

Solh, S. A., & Abdelaziz, S. (2024). Acoustic Emission technique using time-driven method as a tool for assessing the micro-behavior of dense sand. In *4th Asia-Pacific Conference on Physical Modelling in Geotechnics*. https://doi.org/doi:10.53243/ACPMG2024-52

Solh, S. A., Zeinali, S. M., & Abdelaziz, S. (2025). Acoustic Emissions Characteristics of Dense Sand in Drained and Undrained Triaxial Compression Tests. In *Geotechnical Frontiers 2025* (pp. 318-327). https://doi.org/doi:10.1061/9780784485989.032

Wan, R., & Nicot, F. (2010). *Micromechanics of failure in granular geomaterials*. ISTE.

Wang, C., Du, G., Han, Y., He, K., & Li, E. (2023). Evolution characteristics of acoustic emission and strain energy for deep granite under different damage stages. *Geomechanics and Geophysics for Geo-Energy and Geo-Resources*, *9*(1), 14. https://doi.org/10.1007/s40948-023-00557-9

Zhang, H., Ren, Y. H., Ji, S. S., Liu, X. Y., Li, X. C., Zheng, S. Z., & Cao, Z. X. (2025). Study of the Dynamic Splitting Tensile Mechanical Properties and Damage Evolution of Steel Fiber-Reinforced Recycled-Aggregate Concrete Based on Acoustic Emission Technology. *Journal of Materials in Civil Engineering*, *37*(10). https://doi.org/10.1061/JMCEE7.MTENG-20380